



Study of adsorption kinetic, mechanism, isotherm, thermodynamic, and design models for Cu(II) ions on sulfuric acid-modified Eucalyptus seeds: temperature effect

U. Pearlin Kiruba^a, P. Senthil Kumar^{b,*}, K. Sangita Gayatri^b, S. Shahul Hameed^b,
M. Sindhuja^b, C. Prabhakaran^b

^aEDRC—Civil, Larsen & Toubro Limited, Chennai 600 089, India, Tel. +91 9600003167; email: pearl@lntec.com (U.P. Kiruba)

^bDepartment of Chemical Engineering, SSN College of Engineering, Chennai 603 110, India, Tel. +91 9884823425; email: senthilkumarp@ssn.edu.in (P. Senthil Kumar), Tel. +91 9626513932; email: sangitagayatri@gmail.com (K. Sangita Gayatri), Tel. +91 9094530076; email: shahulhameed1992@gmail.com (S. Shahul Hameed), Tel. +91 9626513932; email: sindhujamanohar@yahoo.com (M. Sindhuja), Tel. +91 9600859285; email: prabhachemical@gmail.com (C. Prabhakaran)

Received 20 March 2014; Accepted 10 September 2014

ABSTRACT

The present research was investigated to remove the Cu(II) ions from aqueous solution by adsorption technology using surface-modified Eucalyptus seeds (SMES). Adsorption kinetics, mechanism, isotherms, and thermodynamic parameters were estimated. It was found that the adsorption of Cu(II) ions onto SMES follows pseudo-second-order kinetics. Adsorption mechanism was well explained with intraparticle diffusion and Boyd kinetic models. Diffusivity values of the Cu(II) ions to the SMES were estimated at different temperatures. Effective diffusivity values were estimated at 30°C: 1.9297×10^{-11} , 2.1446×10^{-11} , 2.0165×10^{-11} , 2.2440×10^{-11} , and $2.7434 \times 10^{-11} \text{ m}^2 \text{ s}^{-1}$ for an initial Cu(II) ions concentration of 20–100 mg L⁻¹, respectively. Freundlich adsorption isotherm model agreed with the experimental data to a greater extent, showing the multilayer adsorption of Cu(II) ions onto SMES. The maximum monolayer adsorption capacity of SMES for Cu(II) ions was found to be 76.94 mg of Cu(II) ions g⁻¹ of SMES at 30°C. The determinations from the thermodynamic study show that the process was feasible, spontaneous, and exothermic in nature. A single-stage batch adsorber was designed using Freundlich isotherm model, to estimate the amount of adsorbent that was needed to treat the known volume of the effluent.

Keywords: Adsorption; Surface-modified Eucalyptus seeds; Process design; Cu(II) ions; Kinetics; Mechanism

1. Introduction

The presence of heavy metal ions in effluents beyond permissible limits is a serious environmental issue due to its non-biodegradable nature and

possibility of its accumulation in living tissues. The heavy metal ion such as Cu(II) ions is released into the environment via several sources such as electroplating industries, mining activities, and alloy manufacturing units. Though Cu(II) ions are a vital element essential for good health, its ingestion beyond limits can be detrimental to human health. Long-term

*Corresponding author.

exposure and consumption can lead to liver and kidney damage, and chronic copper poisoning can cause Wilson's disease characterized by brain and renal damage [1–3]. The maximum allowable concentration of Cu(II) ions in potable water as stated by Bureau of Indian Standards is 0.05 mg L^{-1} [4]. Therefore, it is very much necessary to remove the excess copper ions before discharging the effluents into the water bodies.

The removal of Cu(II) ions can be effected by several conventional treatment methods such as ion exchange, reverse osmosis, and membrane separation, but major drawbacks prevail in the implementation of these techniques [5–8]. The removal of heavy metal ions using the above-stated methods becomes too expensive and also inefficient when it comes to the existence of metal ions in very low concentrations. Among the conventional methods, adsorption has been proven to be the most versatile technique for the removal of heavy metals from wastewater, the reason being the ease in operation and its efficiency [9,10]. These days activated carbon is used widely as an adsorbent in treating effluents because of its high porosity, large internal surface area, and high mechanical strength. In spite of its widespread application in industries, activated carbon remains to be an expensive material. Hence, it is the need of the hour to investigate and develop a new cost-effective adsorbent to be applied to the effluent treatment.

Recently, several scientists are on the lookout for replacing conventional activated carbon by economically feasible adsorbent obtained from low-cost agricultural waste [11–15]. Locally available natural material in large quantities whose results have been reported as biosorbents includes Banana pith [16], Indian sal bark [17], coir pith [18], rice husk [19], cork powder [20], wheat bran [21], *Azolla filiculoides* [22], carrot residues [23], cassava tuber bark waste [24], bagasse [25], nipa palm shoot biomass [26], peanut husk [27], poplar wood sawdust [28], wheat straw [29], soybean straw [29], corn [29], corn cob [29], walnut hull [30], rice bran [30], wheat bran [30], pecan nut shell [31], bagasse [32], mango peel [33], wheat straw [34], cashew nut shell [35], *Strychnos potatorum* seeds [36], etc.

The present research is to develop an effective low-cost adsorbent from the source of naturally available agricultural waste such as Eucalyptus seeds to replace the existing commercial materials. Eucalyptus seeds were collected, and it was treated with sulfuric acid to modify its surface to increase adsorption ability for the removal of Cu(II) ions from the aqueous solution. The effect of various operating parameters such as solution pH, adsorbent dose, initial Cu(II) ions concentration,

and contact time on adsorption of Cu(II) ions onto the adsorbent was investigated at different temperatures. Adsorption kinetics, isotherms, and thermodynamics were analyzed by fitting the experimental data to the respective adsorption models. Adsorption mechanism was tested by applying the experimental data to the intraparticle diffusion and Boyd kinetic models. Thermodynamic studies were also done to estimate the standard free energy (ΔG°), standard enthalpy change (ΔH°), and entropy change (ΔS°).

2. Experimental

2.1. Adsorbent preparation

Eucalyptus seeds covered by the woody fruit were collected from the Nilgiri hills in Tamil Nadu, India, where Eucalyptus trees grow in great abundance. These seeds were then rinsed with water to remove dust, dried, and finally grounded to get raw Eucalyptus seed powder (RES). This powder was then treated with concentrated sulfuric acid in the ratio of 1:2 by weight basis (dehydration process), and the mixtures were left for 24 h, followed by washing with water till pH reaches 7. This was further dried at 150°C in hot air oven for about 3 h and grounded to a fine powder to obtain the dehydrated biomass called surface-modified Eucalyptus seeds (SMES).

2.2. Adsorbate preparation

All the chemicals used were of analytical reagent grade. Stock solution of 100 mg L^{-1} of Cu(II) ions was prepared from $\text{CuSO}_4 \cdot 5\text{H}_2\text{O}$ (Merck, India) by dissolving it in double-distilled water. Subsequent dilutions of the stock solution was carried out to prepare the desired test solutions of Cu(II) ions, and the range for these ions prepared from standard solution varied between 20 and 100 mg L^{-1} . The pH of each test solution was adjusted to the desired value using 0.1 M NaOH or 0.1 M HCl before mixing the adsorbent.

2.3. Analysis

The concentration of Cu(II) ions in the solution was determined using atomic absorption spectrometer (AAS, SL176 Model, Elico Limited, Chennai, India). The pH of the solution was measured with Hanna pH meter using a combined glass electrode (HI 98107; Hanna Equipment Private Limited, Mumbai, India). To identify the different chemical functional groups present in the RES and SMES, Fourier transform infrared spectroscopic (FT-IR) analysis was carried out using KBr pellets with the spectral range varied from

4,000 to 450 cm^{-1} (PE IR SPECTRUM ASCII PEDS). To analyze the surface morphology of the RES and SMES, a Quanta 200 FEG scanning electron microscope at an accelerating voltage of 30 kV and with the working distance of 50 μm is used.

2.4. Batch adsorption experiments

Batch adsorption experiments were conducted to investigate the efficiency of SMES for the removal of Cu(II) ions from aqueous solutions at optimum conditions of SMES dose of 1 g L^{-1} at a pH of 5, initial Cu(II) ion concentrations ranging from 20 to

100 mg L^{-1} , temperature of 30°C, and equilibrium time of 10 min. These experiments were done by varying pH of the solution, SMES dose, contact time, initial Cu(II) ion concentration, and temperature. In each study, required quantity of SMES was accurately weighed and added to 100 mL of aqueous solution taken in 100-mL conical flasks. The mixture was agitated at 180 rpm in an orbital incubation shaker. The filtrate was separated after the mixture was centrifuged. The Cu(II) ions concentration in the filtrates was analyzed using AAS. The % removal of Cu(II) ions were computed using the data obtained from the batch studies from the following formula:

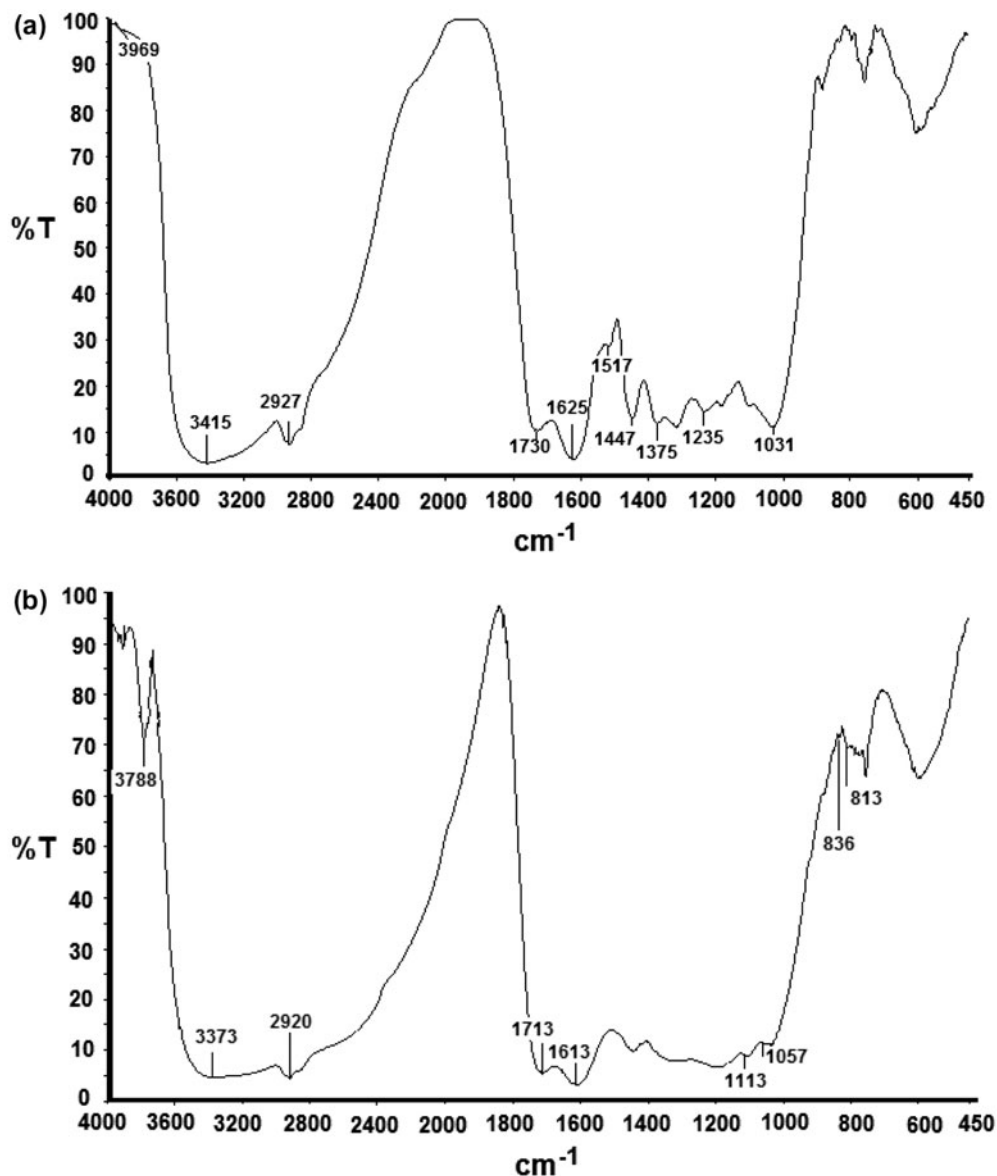


Fig. 1. (a) FT-IR spectrum of RES, (b) FT-IR spectrum of SMES, (c) SEM image of RES, and (d) SEM image of SMES.

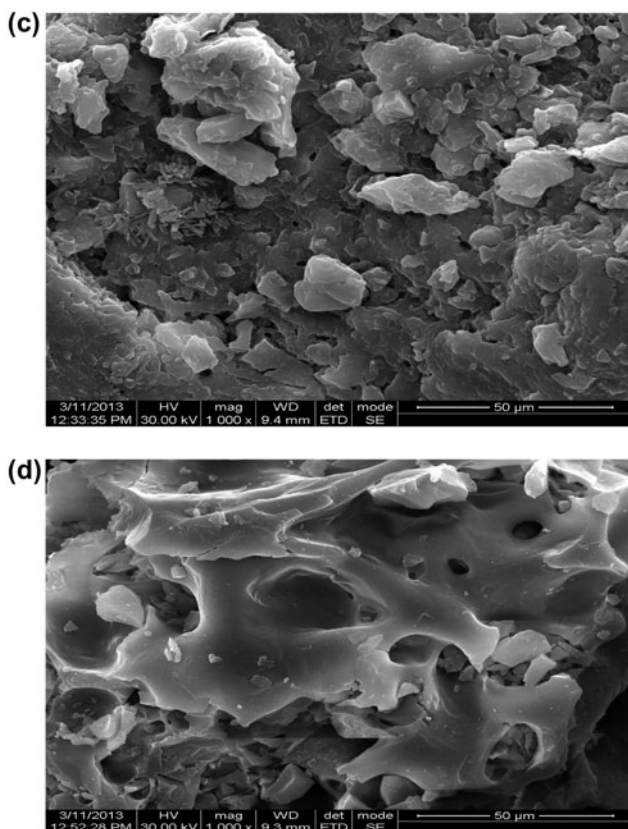


Fig. 1. (Continued).

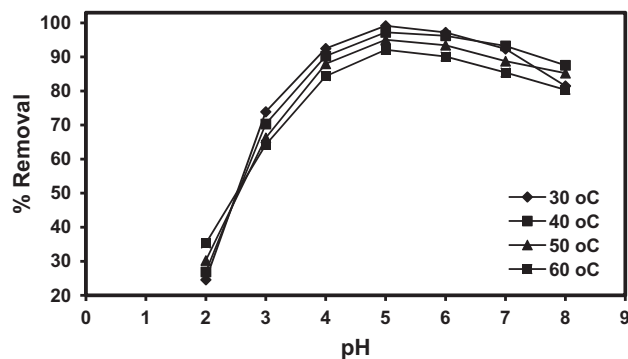


Fig. 2. Effect of pH for adsorption of Cu(II) ions onto SMES (initial Cu(II) ions concentration = 20 mg L⁻¹, SMES dose = 1 g L⁻¹, volume = 100 mL, contact time = 10 min, and temperature = 30–60 °C).

$$\% \text{ Removal} = \frac{C_i - C_f}{C_i} \times 100 \quad (1)$$

where C_i and C_f are the initial and final concentrations (mg L⁻¹) of Cu(II) ions, respectively.

2.5. Adsorption isotherms

A range of solutions of various initial concentrations of Cu(II) ions was prepared, and batch adsorption studies were carried out at different temperatures (30–60 °C) for the purpose of checking the applicability of different adsorption isotherm models such as Langmuir, Freundlich, Temkin, and Dubinin–Radushkevich. The batch studies were done under the following conditions for SMES–Cu(II) ions system: initial solution pH of 5, initial Cu(II) ion concentration in the range of 20–100 mg L⁻¹, SMES dose of 1 g L⁻¹, and contact time of 10 min. To check the adsorption efficiency of SMES, it was compared with the adsorption isotherm of RES–Cu(II) ions adsorption system at 30 °C. To calculate the Cu(II) ions concentration in the solutions, AAS was used to perform the analysis. From the data obtained, adsorption capacity at equilibrium was calculated using the following equation:

$$q_e = \frac{(C_i - C_e)V}{m} \quad (2)$$

where q_e is the amount of Cu(II) ions adsorbed per g of adsorbent (mg g⁻¹), V is the volume of the solution treated (L), C_i is the initial concentration of Cu(II) ions (mg L⁻¹), C_e is the equilibrium Cu(II) ions concentration (mg L⁻¹), and m is the mass of the adsorbent (g).

2.6. Adsorption kinetics

For the purpose of doing kinetic studies, glass equipment with an orbital incubation shaker was used under static conditions. Kinetic investigations were carried out by contacting 1 g L⁻¹ of SMES with 100 mL of Cu(II) ion solution of different concentration ranging from 20 to 100 mg L⁻¹ at different temperatures (30–60 °C). The concentration of Cu(II) ions in the solution was found at known intervals of time, and the analysis of Cu(II) ions content was done using AAS. The amount of Cu(II) ions adsorbed at time t , q_t (mg g⁻¹), was calculated using the following equation:

$$q_t = \frac{(C_i - C_t)V}{m} \quad (3)$$

where C_t is the concentration of Cu(II) ion solution at any time t (mg L⁻¹).

3. Results and discussion

3.1. Characterization of RES and SMES

The FT-IR spectrum of RES is shown in Fig. 1(a). The peak observed at 3,415 cm⁻¹ is due to –OH

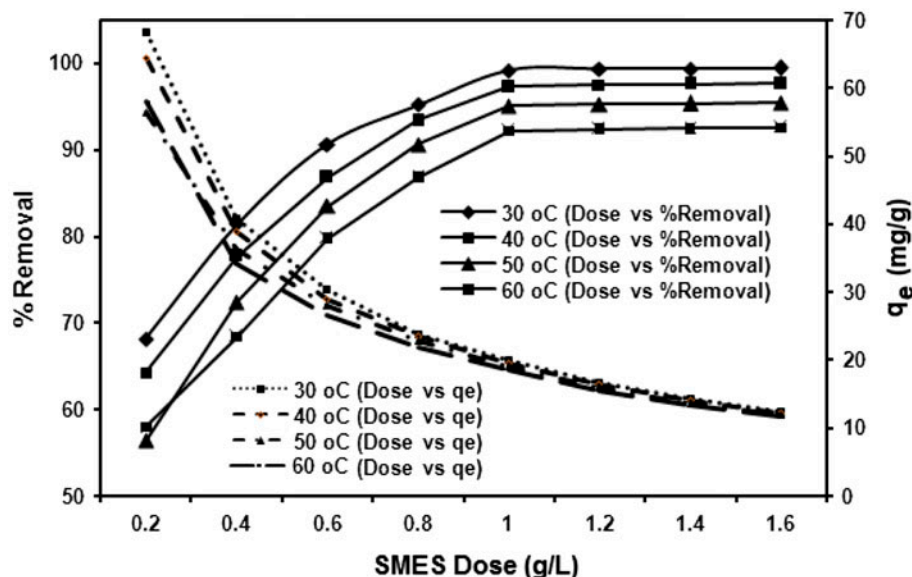


Fig. 3. Effect of SMES dose on Cu(II) ions removal (initial Cu(II) ions concentration = 20 mg L^{-1} , solution pH 5, volume = 100 mL, contact time = 10 min, and temperature = 30–60 °C).

stretching vibration of water and amine. The presence of NH_2 was confirmed by N–H bending vibration at $1,517 \text{ cm}^{-1}$ and C–N stretching vibration at $1,235 \text{ cm}^{-1}$. The presence of water in the RES is further confirmed by the bending vibration observed at $1,625 \text{ cm}^{-1}$. The peak observed at $2,927 \text{ cm}^{-1}$ was due to the $-\text{CH}_2$ vibration of alkyl group. The CH_2 bending vibration is seen to occur at $1,447$ and $1,375 \text{ cm}^{-1}$. The peak at $1,031 \text{ cm}^{-1}$ is due to $-\text{CO}$ stretching vibration of ether groups. Thus, the FT-IR spectrum of RES shows that it mainly carries aliphatic groups with ether and amine linkages. Fig. 1(b) shows the FT-IR spectrum of SMES. Here, the $-\text{OH}$ stretching vibration was found to occur at $3,373 \text{ cm}^{-1}$ and its bending vibration occurs at $1,613 \text{ cm}^{-1}$. The alkyl group $-\text{CH}_2$ stretching vibration was occurred at $2,920 \text{ cm}^{-1}$, and it was found to be slightly lesser than the RES. Carbonyl group C=O presence is evident by the peak observed at $1,713 \text{ cm}^{-1}$. The C–O stretching vibration of ether yields peaks at $1,113$ and $1,057 \text{ cm}^{-1}$. The peaks at 836 and 813 cm^{-1} show cyclic ethers presence as alkyl grouping was nearly absent as their bending vibrations were completely absent, thus establishing carbonization. Thus the results obtained from FT-IR studies indicates that both RES and SMES have a variety of functional groups which may be contributing to the adsorption of Cu(II) ions onto SMES. The change in FT-IR spectrum between SMES and RES is attributed to the effect of sulfuric acid during surface modification. The SEM images of RES and SMES are shown in Fig. 1(c) and (d), respectively. The images show that

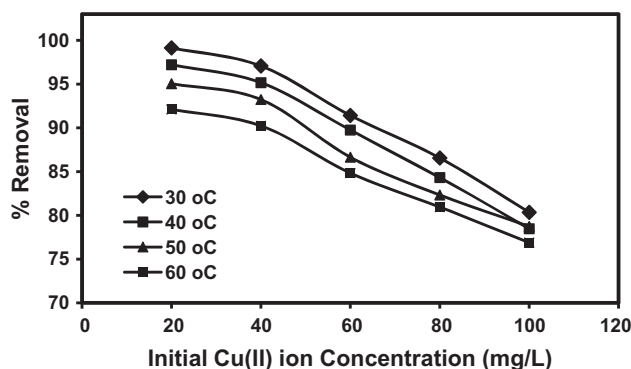


Fig. 4. Effect of initial Cu(II) ions concentration for adsorption of Cu(II) ions onto SMES (initial Cu(II) ions concentration = 20–100 mg L^{-1} , SMES dose = 1 g L^{-1} , solution pH 5, volume = 100 mL, contact time = 10 min, and temperature = 30–60 °C).

the SMES have more porous sites on its surface than RES, indicating that SMES have a greater morphology for Cu(II) ions adsorption.

3.2. Effect of the solution pH

The adsorption of Cu(II) ions as a function of the solution pH is given in Fig. 2. It was observed that the removal of Cu(II) ions increased with increase in the solution pH and then decreased beyond a pH of 5 for all temperatures studied. This is because at lower pH values, the SMES surface becomes more positively

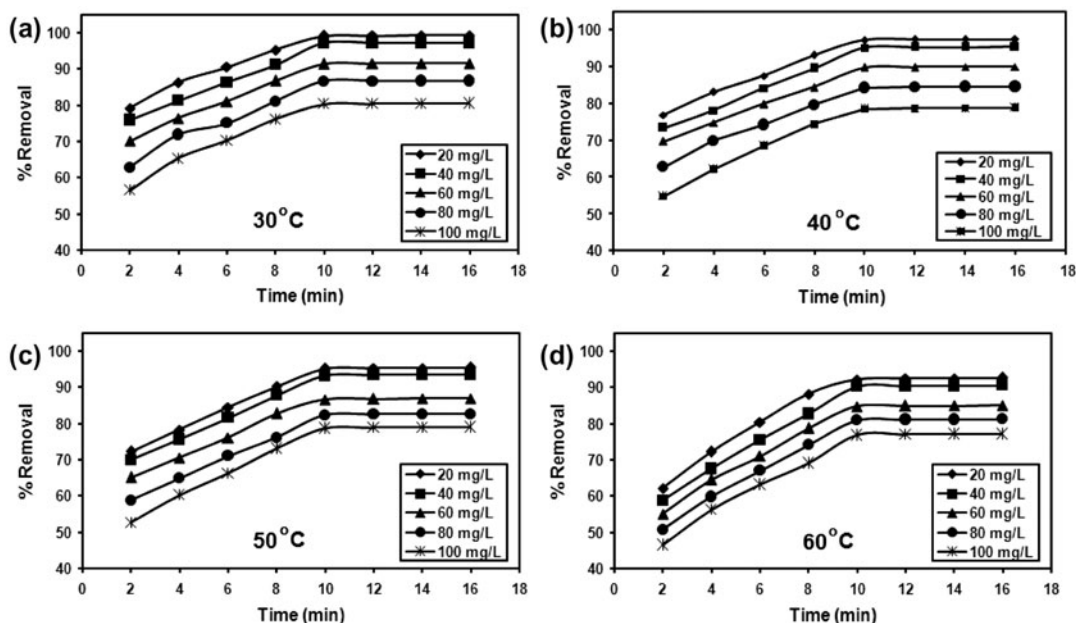


Fig. 5. Effect of contact time for the adsorption of Cu(II) ions onto SMES (initial Cu(II) ions concentration = 20–100 mg L⁻¹, SMES dose = 1 g L⁻¹, solution pH 5, volume = 100 mL, and temperature = 30–60°C).

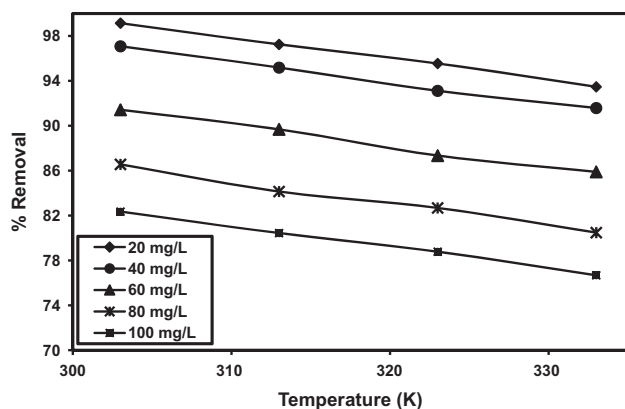


Fig. 6. Effect of temperature on Cu(II) ions removal by SMES (initial Cu(II) ions concentration = 20–100 mg L⁻¹, SMES dose = 1 g L⁻¹, solution pH 5, volume = 100 mL, and contact time = 10 min).

charged, reducing the attraction of Cu(II) ions to the surface. At higher pH values, the SMES surface becomes more negatively charged, thus attracting a greater number of Cu(II) ions. However, a further increase in the solution pH causes the formation of metal hydroxide complexes which decreases the concentration of free Cu(II) ions, thereby causing decrease in the equilibrium adsorption capacity. The maximum adsorption of Cu(II) ions was observed at the solution pH of 5 at 30°C. Hence, pH of 5 was chosen as the

optimum pH for further experimental studies. The effect of the solution pH on metal ions removal can also be discussed with the help of point of zero charge (pH_{pzc}) of the adsorbent material. The surface charge density (σ_o) on SMES was measured using the potentiometric titration method [37]. The point of intersection of surface charge density on SMES against the pH value gives the pH_{pzc} value of 4.3 (figure not shown), which indicates the positive charge on the adsorbent surface below this pH value. Also, if the solution pH is less than the pH_{pzc}, then the predominant metal species will be positively charged [Mⁿ⁺ and M

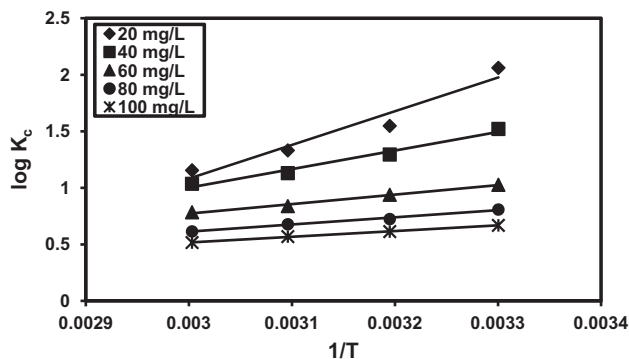


Fig. 7. Thermodynamic study (initial Cu(II) ions concentration = 20–100 mg L⁻¹, SMES dose = 1 g L⁻¹, solution pH 5, volume = 100 mL, and contact time = 10 min).

(OH)⁽ⁿ⁻¹⁾⁺]; thus, the uptake of metal ions in the pH range below pH_{pzc} is a H^+-M^{n+} or $M(OH)^{(n-1)+}$ exchange process. The increase in the solution pH above the pH_{pzc} of the adsorbent material will show a slight increase in the adsorption process, as long as the metal species are positively charged or neutral, even though the adsorbent surface is negatively charged. After certain pH, both the charge on the adsorbent surface and the metal species become negatively charged, and hence, the adsorption process decreased appreciably. At low solution pH, the adsorption was decreased which is mainly due to the higher concentrations of H^+ ions in the solution and which competes with the M^{n+} ions for the adsorption sites on the adsorbent materials. At high solution pH, the adsorption was decreased which is mainly due to the formation of metal hydroxides.

3.3. Effect of the adsorbent dose

Fig. 3 shows the effect of the adsorbent dose on the adsorption of Cu(II) ions onto the SMES surface at different temperatures (30–60°C). The SMES dose is important to determine the capacity of the SMES for adsorption of a given concentration of Cu(II) ions. The adsorbent dose is varied from 0.2 to 1.6 g L⁻¹, and from Fig. 3, it can be seen that initially there is a sharp increase in the % removal of Cu(II) ions as SMES dose is increased, but the equilibrium adsorption capacity (q_e) was decreased. The adsorbent dose becomes almost a constant beyond 1 g L⁻¹ for all temperatures studied. The reason for the increase in percentage removal with increase in the adsorbent dose was attributed to the increase in the number of available active sites with increase in the adsorbent dose, and this reaches a constant value finally which may be due to saturation of the sites. Based on the equilibrium adsorption capacity of the adsorbent, it can be explained that the increase in the adsorbent dose in contact with the fixed concentration and volume of the Cu(II) ions solution caused the reduction in the

amount of Cu(II) ions adsorbed per unit mass of the adsorbent at equilibrium condition. The reason may be attributed to the overlapping or aggregation of adsorption sites, resulting in a decrease in total adsorbent surface area. This problem may be the reason for the interference between the active sites at higher adsorbent dosage or insufficient metal ions in the solution with respect to the available active sites. It is liable that the protons will be combined with the Cu(II) ions for the ligands and thus decreases the interaction between the Cu(II) ions and the adsorbent. Thus the maximum adsorbent efficiency of Cu(II) ions on SMES was found as 99.23% at 1 g L⁻¹ of SMES and at 30°C.

3.4. Effect of the initial Cu(II) ions concentration

The effect of the initial Cu(II) ions concentration on the removal of Cu(II) ions by the SMES experiments was investigated at different temperatures (30–60°C) and at a pH of 5 for the SMES dose of 1 g L⁻¹. Fig. 4 shows that there is a decrease in the % removal of Cu(II) ions with the increase in initial Cu(II) ions concentrations. It was found that the adsorption capacity was increased with the increase in initial Cu(II) ions concentration. The decrease in % removal with the increase in initial Cu(II) ions may be due to the saturation of available active sites on the SMES beyond a particular concentration, and the increase in equilibrium adsorption capacity may be due to the higher adsorption rate and usage of all active sites for adsorption at higher Cu(II) ion concentrations.

3.5. Effect of the contact time

Effect of contact time on the adsorption of Cu(II) ions onto the SMES at different temperatures (30–60°C) was investigated and the results are shown in Fig. 5(a)–(d). The batch studies were carried out for the initial Cu(II) ions concentration range of 20–100 mg L⁻¹ at a pH of 5 and the temperature of 30–60°C. It was observed from the results that the

Table 1
Thermodynamic parameters for the adsorption of Cu(II) ions onto SMES

Initial conc. of Cu(II) ion solution (mg L ⁻¹)	ΔG° (kJ mol ⁻¹)				ΔH° (kJ mol ⁻¹)	ΔS° (J mol ⁻¹ K ⁻¹)
	30°C	40°C	50°C	60°C		
20	-11.959	-9.279	-8.236	-7.368	-57.074	-150.512
40	-8.827	-7.763	-6.992	-6.607	-31.449	-75.156
60	-5.960	-5.627	-5.186	-5.000	-16.059	-33.381
80	-4.692	-4.342	-4.198	-3.922	-12.131	-24.660
100	-3.880	-3.679	-3.523	-3.296	-9.663	-19.082

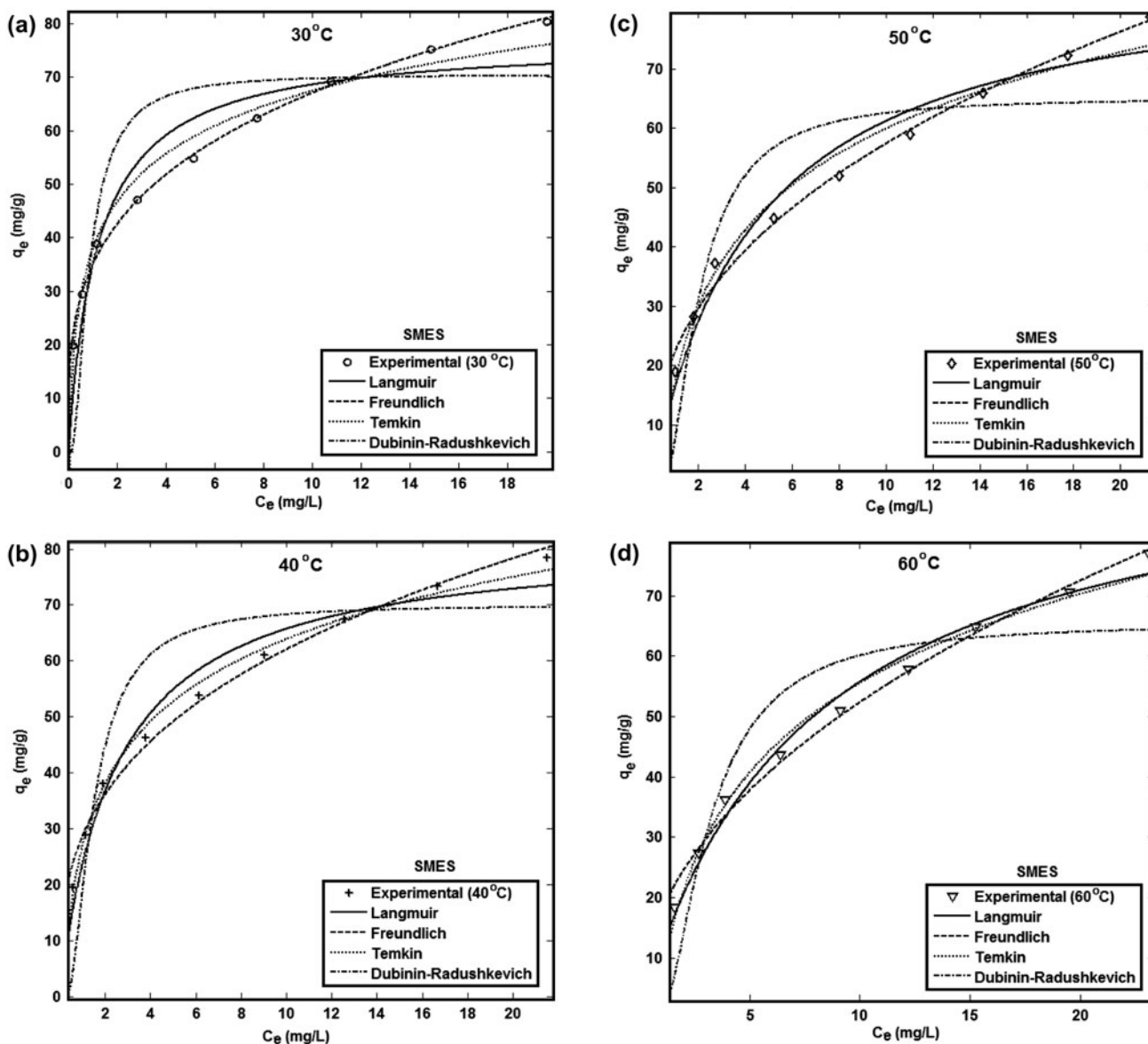


Fig. 8. (a)–(d) The non-linear adsorption isotherm for Cu(II) ions onto SMES (initial Cu(II) ions concentration = 20–100 mg L⁻¹, SMES dose = 1 g L⁻¹, solution pH 5, volume = 100 mL, contact time = 10 min, and temperature = 30–60°C), and (e) the non-linear adsorption isotherm for Cu(II) ions onto RES (initial Cu(II) ions concentration = 10–50 mg L⁻¹, RES dose = 5 g L⁻¹, solution pH 5, volume = 100 mL, contact time = 60 min, and temperature = 30°C).

adsorption of Cu(II) ions onto the SMES increased with increase in the contact time, and it was rapid for the first 8 min, and at 10 min, the equilibrium was almost reached. Further increase in the contact time did not have a significant effect on the % removal of Cu(II) ions. Initially, the large surface area of the

Fig. 8. (Continued).

SMES available could be the reason for the higher adsorption of Cu(II) ions. But later, could have reduced as exhaustion of SMES capacity takes place due to monolayer formation.

3.6. Effect of the temperature

Batch adsorption studies were done at different temperatures of 30, 40, 50, and 60°C for Cu(II) ions concentration range of 20–100 mg L⁻¹ to study the adsorption of Cu(II) ions onto to SMES as a function of the temperature. The adsorbent dose was taken as 1 g L⁻¹, and studies were done at a pH of 5. For rise

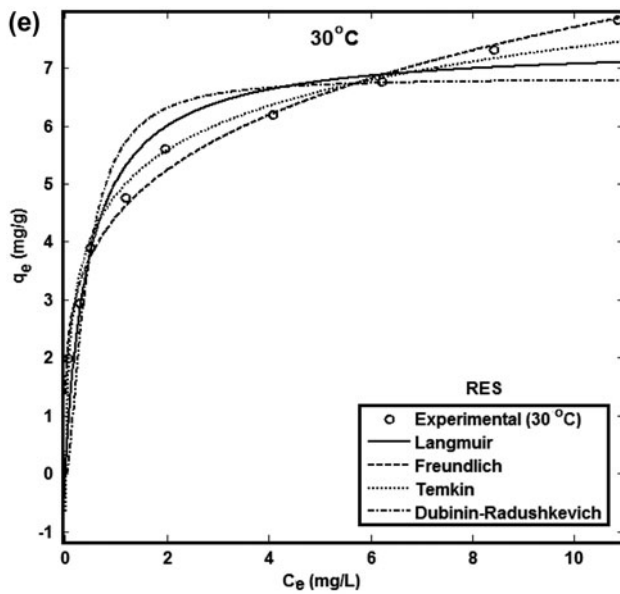


Fig. 8. (Continued).

in the temperature, it was found that the adsorption decreased for the initial Cu(II) ions concentration range of 20–100 mg L⁻¹ as 99.14–93.47%, 97.08–91.58%,

91.42–85.89%, 86.56–80.48%, and 82.35–76.68% as shown in Fig. 6. This shows that there is decrease in the surface activity, and hence, it was inferred that the adsorption of Cu(II) ions onto SMES is an exothermic process. The decrease in the removal of Cu(II) ions with the increase in the temperature may be due to the weakening of adsorptive forces between the active sites of the SMES and Cu(II) ions and also between the adjacent Cu(II) ions of the adsorbed Cu(II) ions in the adsorbent surface. This was further confirmed by fitting the effect of temperature data to the adsorption thermodynamic equations.

3.7. Thermodynamic study

Thermodynamic parameters such as the free energy (ΔG° , kJ mol⁻¹), enthalpy (ΔH° , kJ mol⁻¹), and entropy (ΔS° , J mol⁻¹ K⁻¹) change of adsorption can be calculated from the following equation:

$$\Delta G^\circ = -RT \ln \left(\frac{C_{Ac}}{C_e} \right) = -RT \ln (K_c) \quad (4)$$

$$\log K_c = \frac{\Delta S^\circ}{2.303R} - \frac{\Delta H^\circ}{2.303RT} \quad (5)$$

Table 2

Adsorption isotherm parameters and error values for the adsorption of Cu(II) ions onto the adsorbents

Isotherm model	Parameters	SMES				RES
		Temperature (°C)				
		30	40	50	60	30
Langmuir	q_m (mg g ⁻¹)	76.94	81.82	88.14	97.45	7.401
	K_L (L mg ⁻¹)	0.8396	0.4079	0.2275	0.1337	2.144
	R^2	0.9058	0.9681	0.9643	0.9879	0.9069
	SSE	327.7	105.5	117	38.27	2.997
	RMSE	6.843	3.881	4.088	2.338	0.6543
Freundlich	K_F ((mg g ⁻¹) (L mg ⁻¹) ^(1/n))	35.08	28.66	22.39	17.75	4.44
	n (g L ⁻¹)	3.557	2.981	2.444	2.129	4.178
	R^2	0.9973	0.9936	0.9919	0.9923	0.9891
	SSE	9.229	21.26	26.36	24.25	0.352
	RMSE	1.148	1.743	1.941	1.861	0.224
Temkin	A (L mg ⁻¹)	19.30	5.385	2.542	1.356	78.45
	B	5.561	6.96	8.046	9.25	0.479
	b (kJ mol ⁻¹)	0.453	0.374	0.334	0.299	5.259
	R^2	0.9754	0.9904	0.9802	0.9889	0.9766
	SSE	85.56	31.56	64.81	35.15	0.7539
Dubinin-Radushkevich	RMSE	3.496	2.123	3.043	2.241	0.3282
	$q_{m,D}$ (mg g ⁻¹)	70.45	70.01	65.14	65.46	6.813
	β	3.57×10^{-8}	8.09×10^{-8}	1.33×10^{-7}	2.79×10^{-7}	1.39×10^{-8}
	R^2	0.6909	0.7635	0.7944	0.8283	0.787
	SSE	1,076	780.7	673.2	543.8	7.05
	RMSE	11.6	9.878	9.174	8.245	0.9387

Table 3

Comparison of maximum monolayer adsorption capacity of SMES for Cu(II) ions removal with the various adsorbents at 30°C

Adsorbents	Modifying agent	q_m (mg g ⁻¹)	References
Sugarcane bagasse	Ethylenediamine	139	[25]
Sugarcane bagasse	Triethylenetetramine	133	[25]
Sugarcane bagasse	Sodium bicarbonate	114	[25]
Cassava tuber bark waste	Thioglycolic acid	90.9	[24]
Eucalyptus seeds	Sulfuric acid	76.94	Present study
Nipah palm shoot biomass	Mercaptoacetic acid	66.71	[26]
Azolla filiculoides (aquatic fern)	Hydrogen peroxide–Magnesium chloride	62	[22]
Wheat bran	Sulfuric acid	51.5	[21]
Indian sal bark	Hydrochloric acid	51.4	[17]
Coir pith	Sulfuric acid and ammonium persulphate	39.7	[18]
Carrot residues	Hydrochloric acid	32.74	[23]
Rice husk	Tartaric acid	31.85	[19]
Cork powder	Calcium chloride	15.6	[20]
Banana pith	Nitric acid	13.46	[16]
Peanut husk	Sulfuric acid	10.15	[27]
Raw Eucalyptus seeds	–	7.401	Present study

where K_c is the equilibrium constant, C_e is the equilibrium concentration in solution (mg L⁻¹), C^{Ae} is the amount of Cu(II) ions adsorbed on the adsorbent per liter of solution at equilibrium (mg L⁻¹), R is the gas constant (8.314 J mol⁻¹ K⁻¹), and T is the temperature (K). Adsorption of Cu(II) ions onto the SMES decreased when the temperature was increased from 303 to 333 K as shown in Fig. 6. The values of ΔH° and ΔS° were calculated from the slope and the intercept from the plot of $\log K_c$ vs. $1/T$ (Fig. 7). The plots helped to compute the values of the thermodynamic parameter as shown in Table 1. It was observed that the ΔG° is small and negative but increases with increase in temperature showing that the adsorption process is feasible and spontaneous. This also indicates that the adsorption process becomes more favorable at lower temperatures. The values of ΔG° may also predict the type of adsorption process. The importance of ΔG° is given as follows: for physical adsorption: -20 to 0 kJ mol⁻¹; chemical adsorption: -80 to -400 kJ mol⁻¹. For the present adsorption system, the values of ΔG° were observed between -20 and 0 kJ mol⁻¹ for all studied temperature and which indicates that the present adsorption system was a physical process. Negative ΔH° values shows that the adsorption is exothermic in nature which may due to the weak force of attraction between the Cu(II) ions and the adsorbent surface. The ΔS° value helps us to describe the randomness at the SMES solution interface during the process.

3.8. Adsorption isotherms

The adsorption isotherm models such as Langmuir [38], Freundlich [39], Dubinin–Radushkevich [40], and Temkin [41] were used to study the effect of initial Cu (II) ions concentration at different temperatures (30–60°C), and the results are shown in Fig. 8(a)–(d).

The nonlinear form of the Langmuir equation is given by:

$$q_e = \frac{q_m K_L C_e}{1 + K_L C_e} \quad (6)$$

The nonlinear form of Freundlich adsorption isotherm equation is given by:

$$q_e = K_F C_e^{1/n} \quad (7)$$

The nonlinear form of Dubinin–Radushkevich adsorption isotherm model is given as:

$$q_e = q_{m,D} \exp \left(-\beta \left(RT \ln \left(1 + \frac{1}{C_e} \right) \right)^2 \right) \quad (8)$$

and the mean free energy, E of adsorption per molecule of the copper ions can be calculated from the equation:

$$E = \frac{1}{\sqrt{2\beta}} \quad (9)$$

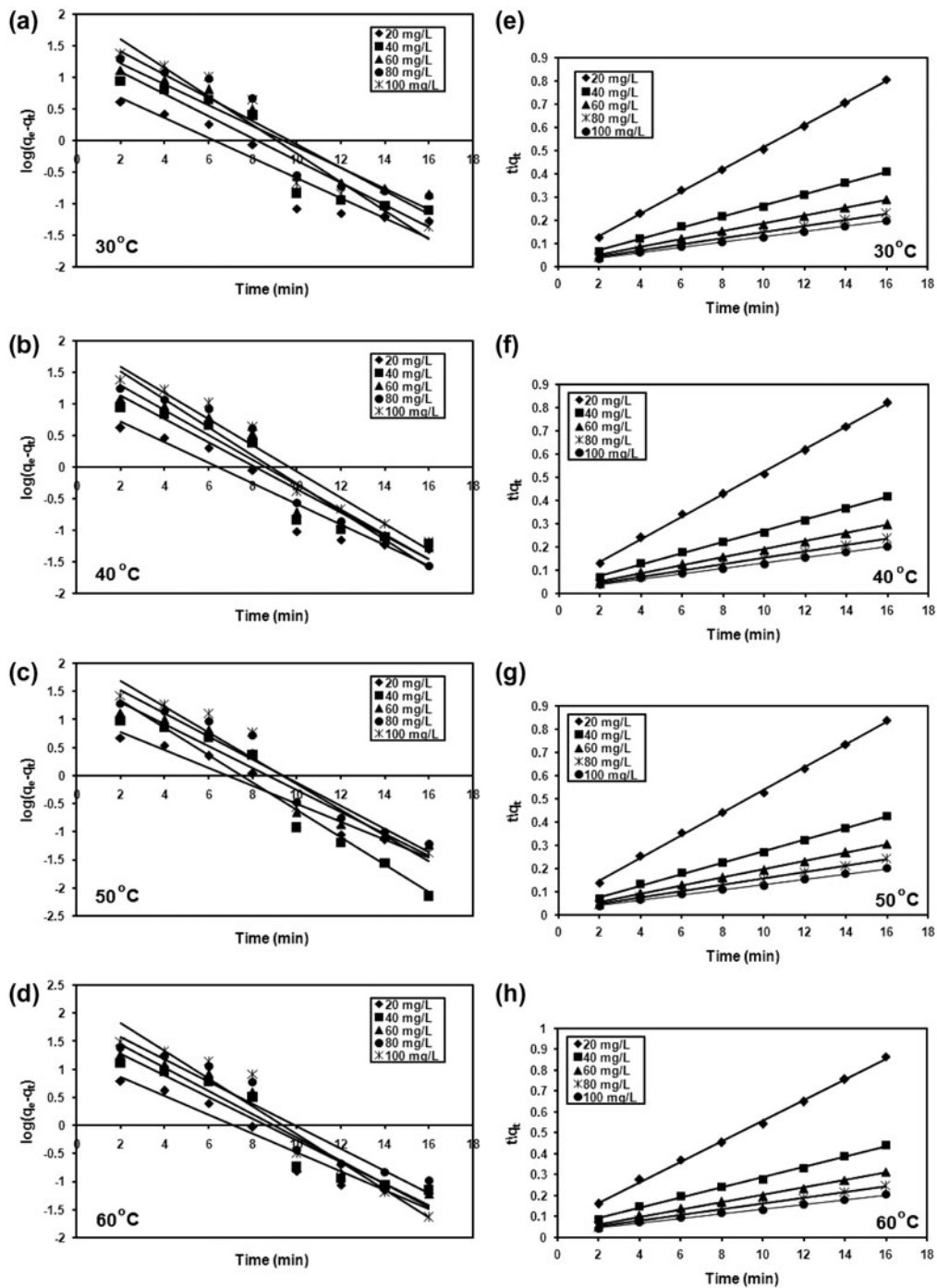


Fig. 9. (a)–(h) Adsorption kinetic plots for adsorption of Cu(II) onto SMES (initial Cu(II) ions concentration = 20–100 mg L⁻¹, SMES dose = 1 g L⁻¹, solution pH 5, volume = 100 mL, and temperature = 30–60°C).

The Temkin isotherm equation is given as follows:

$$q_e = B \ln(A C_e) \quad (10)$$

where q_e is the adsorption capacity at equilibrium (mg g⁻¹), q_m is the maximum monolayer adsorption capacity (mg g⁻¹), K_L is the Langmuir constant related to the affinity of Cu(II) ions to the SMES (L mg⁻¹), C_e

Table 4

Comparison between the adsorption rate constants, q_e estimated and correlation coefficients for pseudo-first-order and pseudo-second-order rate equations

Temp (°C)	Conc. of Cu(II) ions solution (mg L ⁻¹)	Kinetic model							
		Pseudo-first-order equation			Pseudo-second-order equation				
		k_1 (min ⁻¹)	q_e, cal (mg g ⁻¹)	R^2	k_2 (g mg ⁻¹ min ⁻¹)	q_e, cal (mg g ⁻¹)	h (mg g ⁻¹ min ⁻¹)	q_e, exp (mg g ⁻¹)	R^2
30	20	0.365	9.761	0.899	0.0632	20.921	27.701	19.912	0.998
	40	0.405	27.688	0.889	0.0250	41.494	43.103	38.977	0.998
	60	0.381	36.166	0.905	0.0172	58.824	59.524	55.122	0.999
	80	0.424	61.390	0.899	0.0114	75.188	64.516	69.531	0.998
	100	0.519	112.15	0.934	0.0114	87.719	71.429	80.562	0.998
40	20	0.373	11.015	0.911	0.0576	20.833	25	19.542	0.999
	40	0.426	31.405	0.903	0.0230	41.666	40	38.213	0.998
	60	0.454	49.431	0.915	0.0170	58.823	58.824	54.042	0.998
	80	0.509	90.573	0.946	0.0131	71.429	66.667	67.723	0.998
	100	0.474	100	0.953	0.0103	83.333	71.429	78.895	0.998
50	20	0.366	12.445	0.915	0.0465	20.747	20	19.131	0.998
	40	0.559	66.527	0.944	0.0218	40.486	35.714	37.415	0.998
	60	0.449	50.234	0.934	0.0161	57.143	52.632	52.512	0.998
	80	0.474	87.096	0.931	0.0112	70.423	55.556	66.197	0.997
	100	0.527	142.23	0.931	0.0086	82.645	58.824	79.012	0.996
60	20	0.385	15.596	0.937	0.0353	20.408	14.706	18.576	0.998
	40	0.442	46.345	0.907	0.0142	40.323	23.089	36.278	0.996
	60	0.477	72.111	0.910	0.0109	56.179	34.483	51.078	0.996
	80	0.456	94.624	0.920	0.0079	70.922	40	65.121	0.996
	100	0.571	211.35	0.939	0.0064	82.305	43.478	77.213	0.995

is the concentration of the Cu(II) ions in the solution at equilibrium (mg L⁻¹), C_0 is the initial Cu(II) ions concentration in the solution (mg L⁻¹), K_F is the Freundlich constant ((mg g⁻¹) (L mg⁻¹)^(1/n)) related to the bonding energy, n is a measure of the deviation from the linearity of adsorption (g L⁻¹), $q_{m,D}$ is the Dubinin–Radushkevich monolayer adsorption capacity (mg g⁻¹), β is a constant related to adsorption energy, R is the gas constant (8.314 J mol⁻¹ K), T is the temperature (K), E is the mean free energy (kJ mol⁻¹), A is the equilibrium binding constant (L mg⁻¹) corresponding to the maximum binding energy, $B = RT/b$, is the constant related to the heat of adsorption, and b is the heat of adsorption (J mol⁻¹).

The adsorption isotherm parameters, error values (SSE, sum of squared error and RMSE, root mean squared error), and coefficient of determination (R^2) values were estimated from the plot of C_e vs. q_e (Fig. 8(a)–(d)), and the values are given in Table 2. The isotherm model for which R^2 is closer to 1 in comparison with other models is chosen as the one that better fits the experimental data. The experimental data gave results for the following isotherms

in the order: Freundlich > Temkin > Langmuir > Dubinin–Radushkevich, based on R^2 values. Table 2 clearly shows that the experimental data are well described by the Freundlich adsorption isotherm model ($R^2 = 0.9962$) better than the Langmuir, Temkin, and Dubinin–Radushkevich adsorption isotherm models. This shows that adsorption of Cu(II) ions onto the SMES may be due to multilayer adsorption. The Freundlich adsorption isotherm model is an indication of the surface heterogeneity of the adsorbent. This leads to the conclusion that the surface of the adsorbent is made of heterogeneous patches which is favorable for the adsorption phenomenon.

The comparison of maximum monolayer adsorption capacity (q_m) for Cu(II) ions onto SMES with other adsorbents is shown in Table 3. It can be seen that SMES studied in this work has a large maximum monolayer adsorption capacity.

3.9. Adsorption kinetics

The prediction of the adsorption kinetics is an important step for the design of an adsorption system.

Table 5

Comparison of parameters for different adsorption mechanism models for adsorption of Cu(II) ions onto SMES

Temp (°C)	Conc. of Cu(II) ions solution (mg L ⁻¹)	Intraparticle diffusion model			Boyd kinetic model		
		k_p (mg g ⁻¹ min ^{1/2})	C (mg g ⁻¹)	R^2	B	D_i ($\times 10^{-11}$ m ² s ⁻¹)	R^2
30	20	1.623	14.025	0.912	0.365	1.9297	0.899
	40	3.645	25.662	0.929	0.405	2.1446	0.889
	60	5.3812	35.53	0.922	0.381	2.0165	0.905
	80	7.7446	41.435	0.917	0.424	2.2440	0.899
	100	9.6247	46.007	0.906	0.519	2.7434	0.934
40	20	1.706	13.33	0.917	0.374	1.9748	0.911
	40	3.795	24.38	0.924	0.426	2.2535	0.903
	60	5.174	35.20	0.927	0.453	2.3964	0.925
	80	7.179	41.74	0.922	0.509	2.6926	0.946
	100	9.863	43.39	0.909	0.475	2.5128	0.953
50	20	1.948	12.03	0.919	0.368	1.9467	0.915
	40	4.036	22.78	0.923	0.561	2.9677	0.944
	60	5.558	32.10	0.913	0.450	2.3805	0.934
	80	8.088	36.78	0.928	0.474	2.5075	0.931
	100	11.02	39.17	0.919	0.528	2.7931	0.931
60	20	2.542	9.750	0.896	0.385	2.0367	0.937
	40	5.309	17.02	0.923	0.443	2.3435	0.907
	60	7.406	24.34	0.916	0.477	2.5233	0.910
	80	10.12	28.47	0.922	0.457	2.4175	0.920
	100	12.61	31.58	0.924	0.571	3.0206	0.939

The adsorption rate constants and the order of adsorption rate kinetics are important physico-chemical parameters to evaluate the basic qualities of the good adsorbent. The data obtained from the effect of contact time on the adsorption process can be used to find whether the adsorption of Cu(II) ions onto SMES follows pseudo-first-order [42] or pseudo-second-order [43] kinetics.

The pseudo-first-order kinetic model is given by the following equation:

$$\log(q_e - q_t) = \log q_e - \frac{k_1}{2.303} t \quad (12)$$

And pseudo-second-order kinetic model is given by the following equation:

$$\frac{t}{q_t} = \frac{1}{k_2 q_e^2} + \frac{1}{q_e} t \quad (13)$$

where q_e is the adsorption capacity of Cu(II) ions onto SMES at equilibrium time (mg g⁻¹), q_t is the adsorption capacity of Cu(II) ions onto SMES at time t (mg g⁻¹), t is time (min), k_1 is pseudo-first-order rate constant (min⁻¹), k_2 is pseudo-second-order rate constant (g mg⁻¹ min⁻¹), and $h = k_2 q_e^2$ is the initial

adsorption rate (mg g⁻¹ min⁻¹). The kinetic parameters and other values were calculated from the linear plots of the Eqs. (12) (Fig. 9(a)–(d)) and (13) (Fig. 9(e)–(h)), and the values are listed in Table 4.

From Table 4, it was observed that the better R^2 values were observed for the pseudo-second-order kinetic model than the pseudo-first-order kinetic model, which indicates that the pseudo-second-order kinetic model fits the adsorption kinetic data better than the pseudo-first-order kinetic model. Moreover, the comparison between the calculated adsorption capacity values (q_e cal) from the pseudo-second-order kinetic model are very close to the experimentally calculated adsorption capacity (q_e exp) values (Table 4). This confirms that the adsorption of Cu(II) ions onto SMES follows the pseudo-second-order kinetic model and the adsorption rate may be controlled by chemical adsorption involving the valency forces through sharing or exchange of electrons between the adsorbent and adsorbate which provides the best correlation of the experimental data [42]. Also, the pseudo-second-order rate constant (k_2) values were found to be decreased with the increase in initial Cu(II) ions concentrations, that is, the time needed for the equilibrium adsorption increased with small differences as the initial Cu(II) ions concentration increased.

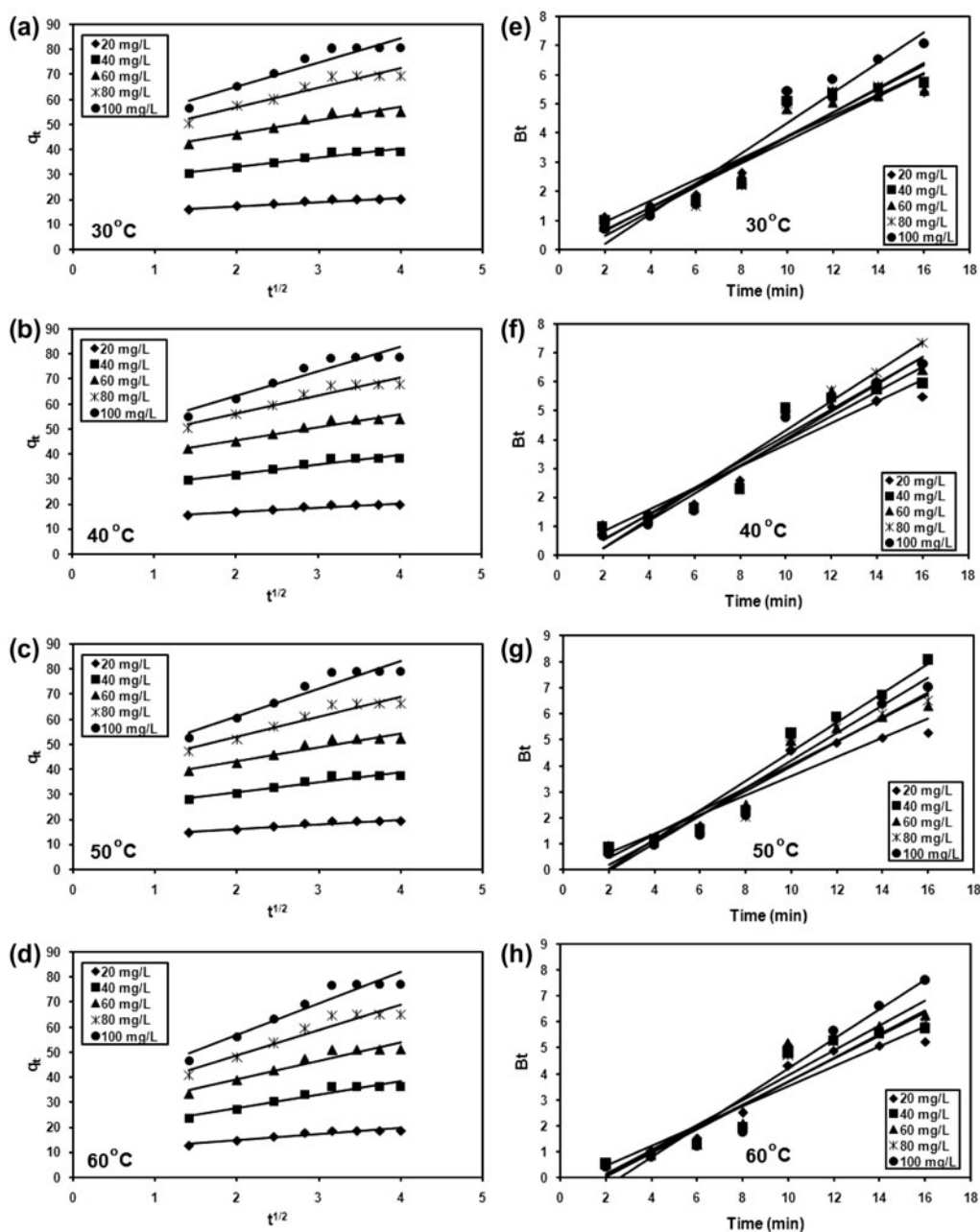


Fig. 10. (a)–(h) Adsorption mechanism plots for the adsorption of Cu(II) onto SMES (initial Cu(II) ions concentration = 20–100 mg L⁻¹, SMES dose = 1 g L⁻¹, solution pH 5, volume = 100 mL, and temperature = 30–60°C).

3.10. Adsorption mechanism

The adsorption of Cu(II) ions onto SMES is a solid–liquid adsorption process which is characterized by film diffusion (external diffusion), intraparticle diffusion (internal diffusion), or both. The kinetic models only show us whether adsorption process follows pseudo-first-order or pseudo-second-order kinetics. But, in order to find the adsorption mechanism and

rate controlling steps in the removal of Cu(II) ions by SMES, it is important to use models such as Weber and Morris intraparticle diffusion model [44] and Boyd kinetic model [45].

The Weber and Morris intraparticle diffusion model can be represented as shown below:

$$q_t = k_p t^{1/2} + C \tag{14}$$

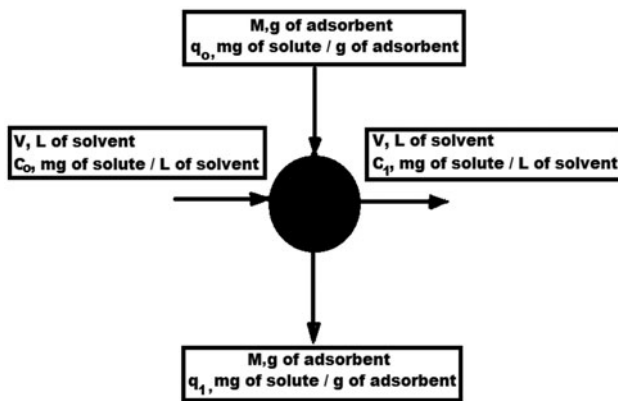


Fig. 11. Schematic diagram of a single-stage batch adsorber.

where q_t is the adsorption capacity at time t (mg g^{-1}), k_p is the intraparticle diffusion rate constant ($\text{mg g}^{-1} \text{min}^{0.5}$), t is the time (min), and C is the film thickness. The values of k_p , C , and R^2 were calculated from the linear plot of Eq. (14), and the values are shown in Table 5. Fig. 10(a)–(d) show that for wide range of contact time between Cu(II) ion and SMES, the plot is linear but does not pass through origin. This indicates that intraparticle diffusion is not only the rate-controlling step and even other steps might be involved simultaneously.

The Boyd kinetic model is given by the relation:

$$F = 1 - \frac{6}{\pi^2} \exp(-Bt) \quad (15)$$

The above expression can be rewritten as:

$$Bt = -0.4977 - \ln(1 - F) \quad (16)$$

where F is the fraction of Cu(II) ions adsorbed at any time t and is given by the relation:

$$F = \frac{q_t}{q_e} \quad (17)$$

and q_t is the Cu(II) ions adsorbed at any time t , q_e is the Cu(II) ions adsorbed at equilibrium time, and Bt is the mathematical function of F . Fig. 10(e)–(h) show that the plots are linear but does not pass through origin, which indicates that adsorption process is controlled by film diffusion. The effective diffusion coefficient, D_i ($\text{m}^2 \text{s}^{-1}$), is calculated using the following equation:

$$B = \frac{\pi^2 D_i}{r^2} \quad (18)$$

where r is the radius of the SMES particles (m). The values of B , D_i , and R^2 are presented in Table 5. From the results observed, it was indicated that the

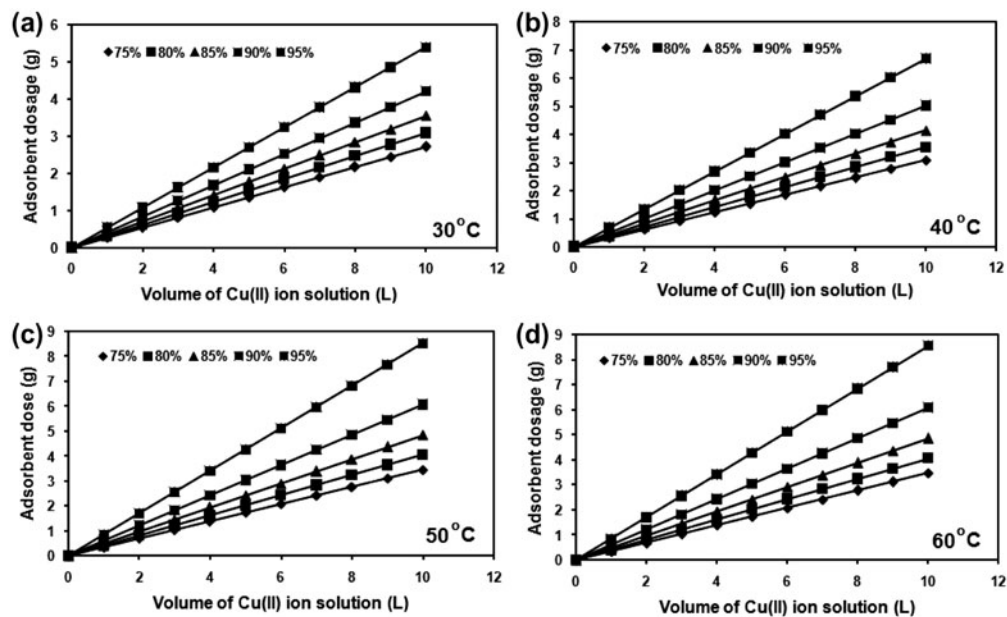


Fig. 12. Design results of a single-stage batch adsorber.

adsorption of Cu(II) ions onto SMES was controlled by both film and intraparticle diffusion.

3.11. Design of a single-stage batch adsorber

The best-fitted adsorption isotherm model data were used to design a single-stage adsorber to estimate the amount of adsorbent needed to treat the desired volume of the desired initial Cu(II) ions concentration. A schematic diagram of a single-stage batch adsorber is shown in Fig. 11. The design objective was to reduce the concentration of Cu(II) ions from C_0 (mg L^{-1}) to C_e (mg L^{-1}) of the solution volume V (L), and the capacity of the adsorbent was changed from q_0 (mg g^{-1}) to q_e (mg g^{-1}). The mass balance for a single-stage batch adsorber at equilibrium condition is given as follows (at time $t = 0$, $q_0 = 0$):

$$V(C_0 - C_e) = M(q_e - q_0) = Mq_e \quad (19)$$

where M is the mass of the adsorbent (g). The adsorption isotherm data fit the Freundlich adsorption isotherm model well for Cu(II) ions–SMES system, and the Freundlich equation was used for the design of a single-stage batch adsorber. The above Eq. (19) was rearranged, and the following expression was obtained:

$$M = \frac{(C_0 - C_e)}{q_e} V = \frac{(C_0 - C_e)}{K_F C_e^{1/n}} V \quad (20)$$

The plot of mass of adsorbent vs. volume of the solution of initial Cu(II) ions concentration of 20 mg L^{-1} for 75, 80, 85, 90, and 95% of Cu(II) ions removal at different solution volumes (1–10 L) for a single-stage batch adsorber, for which the design procedure is outlined (Fig. 12(a)–(d)). The present design was used to estimate the amount of adsorbent dose that was required for the treatment of known volume of effluents.

4. Conclusion

The present investigation shows that the SMES are an effective adsorbent for the removal of Cu(II) ions from aqueous solutions. The results obtained from FT-IR spectrum and SEM analysis indicated that the SMES can be used as an adsorbent for Cu(II) ions removal. The adsorption of Cu(II) ions onto the SMES was found to be influenced by several factors such as pH of the solution, adsorbent dose, initial Cu(II) ion

concentration, contact time, and temperature. It was found that the adsorption of Cu(II) ions was highly dependent on pH and the removal of the ions increased with increase in pH and then was found to decrease. The percentage removal of Cu(II) ions was found to increase with increase in adsorbent dose and decrease with increase in initial Cu(II) ion concentration. With respect to contact time, the percentage removal increased up to a time of 10 min and almost remained constant for further increase in time. The experimental data were analyzed by the various adsorption isotherms such as Langmuir, Freundlich, Temkin, and Dubinin–Radushkevich isotherms. The characteristic parameters for each isotherm and related correlation coefficients were computed. The experimental data yielded excellent fits for the isotherm models in the order: Freundlich > Temkin > Langmuir > Dubinin–Radushkevich based on its correlation coefficient values. The temperature and thermodynamic studies showed that the system is spontaneous and exothermic. The adsorption kinetics was studied by applying the experimental data to the pseudo-first-order and pseudo-second-order kinetic models, and it was found that the adsorption of Cu(II) ions onto SMES follows pseudo-second-order kinetics. The adsorption mechanism was explained with the intraparticle diffusion and Boyd kinetic models and which confirms that the adsorption of Cu(II) ions onto the SMES was controlled by both film and particle diffusion. Also, a single-stage batch adsorber was designed to estimate the quantity of adsorbent dose that was needed to treat the known volume of the effluent. Based on the results observed, it can be concluded that the SMES can act as an excellent adsorbent for the removal of heavy metal ions from the wastewater.

Acknowledgements

The authors are grateful for the financial support from the SSN Trust, Chennai.

References

- [1] H.K. Chuttani, P.S. Gupta, S. Gulati, D.N. Gupta, Acute copper sulphate poisoning, *Ame. J. Med.* 39 (1965) 849–854.
- [2] I. Bremner, Copper toxicity studies using domestic and laboratory animals, in: J.O. Nriagu (Ed.), *Copper in the Environment. Part II: Health Effects*, Wiley, New York, NY, 1979, pp. 285–306.
- [3] A. Demayo, M.C. Taylor, K.W. Taylor, G.B. Wiersma, Effects of copper on humans, laboratory and farm animals, terrestrial plants, and aquatic life, *CRC Crit. Rev. Environ. Control* 12 (1982) 183–255.

- [4] BIS, Methods of Sampling and Test (Physical and Chemical) for Water and Waste Water: Part 42 Copper (first revision), IS No. 3025 (Part 42), 1992.
- [5] S.S. Banerjee, M.V. Joshi, R.V. Jayaram, Removal of Cr(VI) and Hg(II) from aqueous solutions using fly ash and impregnated fly ash, *Sep. Sci. Technol.* 39 (2004) 1611–1629.
- [6] D.N. Bennion, J. Newman, Electrochemical removal of copper ions from very dilute solutions, *J. Appl. Electrochem.* 2 (1972) 113–122.
- [7] H.S. Murlidhara, *Advances in Solid-Liquid Separation*, Batelle Press, Columbus Richland, OH, 1996.
- [8] E.S. Tarleton, The role of field-assisted techniques in solid/liquid separation, *Filtr. Sep.* 29 (1992) 246–252.
- [9] Z. Aksu, F. Gönen, Z. Demircan, Biosorption of chromium(VI) ions by Mowital®B30H resin immobilized activated sludge in a packed bed: Comparison with granular activated carbon, *Proc. Biochem.* 38 (2002) 175–186.
- [10] M. Corapcioglu, C.P. Huang, The adsorption of heavy metals onto hydrous activated carbon, *Water Res.* 21 (1987) 1031–1044.
- [11] M. Weltrowski, B. Martel, M. Morcellet, Chitosan N-benzyl sulfonate derivatives as sorbents for removal of metal ions in an acidic medium, *J. Appl. Polym. Sci.* 59 (1996) 647–654.
- [12] S.E. Bailey, T.J. Olin, R.M. Bricka, D.D. Adrian, A review of potentially low-cost sorbents for heavy metals, *Water Res.* 33 (1999) 2469–2479.
- [13] G. McKay, Y.S. Ho, J.C.Y. Ng, Biosorption of copper from waste waters: A review, *Sep. Purif. Methods* 28 (1999) 87–125.
- [14] J.C. Igwe, A.A. Abia, A bioseparation process for removing heavy metals from waste water using biosorbents, *Afr. J. Biotechnol.* 5 (2006) 1167–1179.
- [15] W.S.W. Ngah, M.A.K.M. Hanafiah, Removal of heavy metal ions from wastewater by chemically modified plant wastes as adsorbents: A review, *Bioresour. Technol.* 99 (2008) 3935–3948.
- [16] K.S. Low, C.K. Lee, A.C. Leo, Removal of metals from electroplating wastes using banana pith, *Bioresour. Technol.* 51 (1995) 227–231.
- [17] B.R. Reddy, N. Mirghaffari, I. Gaballah, Removal and recycling of copper from aqueous solutions using treated Indian barks, *Resour. Conserv. Recy.* 21 (1997) 227–245.
- [18] C. Namasivayam, K. Kadirvelu, Agricultural solid wastes for the removal of heavy metals: Adsorption of Cu(II) by coirpith carbon, *Chemosphere* 34 (1997) 377–399.
- [19] K.K. Wong, C.K. Lee, K.S. Low, M.J. Haron, Removal of Cu and Pb by tartaric acid modified rice husk from aqueous solutions, *Chemosphere* 50 (2003) 23–28.
- [20] N. Chubar, J.R. Carvalho, M.J.N. Correia, Heavy metals biosorption on cork biomass: Effect of the pre-treatment, *Colloids Surf., A* 238 (2004) 51–58.
- [21] A. Özer, D. Özer, A. Özer, The adsorption of copper (II) ions onto dehydrated wheat bran (DWB): Determination of equilibrium and thermodynamic parameters, *Process Biochem.* 39 (2004) 2183–2191.
- [22] M.T. Ganji, M. Khosravi, R. Rakhshaei, Biosorption of Pb, Cd, Cu and Zn from wastewater by treated *Azolla filiculoides* with H₂O₂/MgCl₂, *Int. J. Environ. Sci. Technol.* 1 (2005) 265–271.
- [23] B. Nasernejad, T.E. Zadeh, B.B. Pour, M.E. Bygi, A. Zamani, Comparison for biosorption modeling of heavy metals (Cr(III), Cu(II), Zn(II)) adsorption from wastewater by carrot residues, *Process Biochem.* 40 (2005) 1319–1322.
- [24] M. Horsfall, A.A. Abia, A.I. Spiff, Kinetic studies on the adsorption of Cd²⁺, Cu²⁺ and Zn²⁺ ions from aqueous solutions by cassava (*Manihot sculenta* Cranz) tuber bark waste, *Bioresour. Technol.* 97 (2006) 283–291.
- [25] O.K. Junior, L.V.A. Gurgel, J.C.P. de Melo, V.R. Botaro, T.M.S. Melo, R.P. de Freitas Gil, L.F. Gil, Adsorption of heavy metal ion from aqueous single metal solution by chemically modified sugarcane bagasse, *Bioresour. Technol.* 98 (2006) 1291–1297.
- [26] D. Wankasi, M. Horsfall Jr., A.I. Spiff, Sorption kinetics of Pb²⁺ and Cu²⁺ ions from aqueous solution by Nipah palm (*Nypa fruticans* Wurmb) shoot biomass, *Electron. J. Biotechnol.* 9 (2006) 587–592.
- [27] Q. Li, J. Zhai, W. Zhang, M. Wang, J. Zhou, Kinetic studies of adsorption of Pb(II), Cr(III) and Cu(II) from aqueous solution by sawdust and modified peanut husk, *J. Hazard. Mater.* 141 (2006) 163–167.
- [28] M. Šćiban, B. Radetić, Z. Kevrešan, M. Klačnja, Adsorption of heavy metals from electroplating wastewater by wood sawdust, *Bioresour. Technol.* 98 (2007) 402–409.
- [29] M. Šćiban, M. Klačnja, B. Škrbić, Adsorption of copper ions from water by modified agricultural by-products, *Desalination* 229 (2008) 170–180.
- [30] X. Wang, Z.Z. Li, C. Sun, A comparative study of removal of Cu(II) from aqueous solutions by locally low-cost materials: Marine macroalgae and agricultural by-products, *Desalination* 235 (2009) 146–159.
- [31] J.C.P. Vaghetti, E.C. Lima, B. Royer, B.M. da Cunha, N.F. Cardoso, J.L. Brasil, S.L.P. Dias, Pecan nutshell as biosorbent to remove Cu(II), Mn(II) and Pb(II) from aqueous solutions, *J. Hazard. Mater.* 162 (2009) 270–280.
- [32] Y. Jiang, H. Pang, B. Liao, Removal of copper(II) ions from aqueous solution by modified bagasse, *J. Hazard. Mater.* 164 (2009) 1–9.
- [33] M. Iqbal, A. Saeed, I. Kalim, Characterization of adsorptive capacity and investigation of mechanism of Cu²⁺, Ni²⁺ and Zn²⁺ adsorption on mango peel waste from constituted metal solution and genuine electroplating effluent, *Sep. Sci. Technol.* 44 (2009) 3770–3791.
- [34] V.B.H. Dang, H.D. Doan, T. Dang-Vu, A. Lohi, Equilibrium and kinetics of biosorption of cadmium(II) and copper(II) ions by wheat straw, *Bioresour. Technol.* 100 (2009) 211–219.
- [35] P.S. Kumar, S. Ramalingam, V. Sathyaselvabala, S.D. Kirupha, S. Sivanesan, Removal of copper(II) ions from aqueous solution by adsorption using cashew nut shell, *Desalination* 266 (2011) 63–71.
- [36] P.S. Kumar, A.S.L.S. Deepthi, R. Bharani, C. Prabhakaran, Adsorption of Cu(II), Cd(II) and Ni(II) ions from aqueous solution by unmodified *Strychnos potatorum* seeds, *Eur. J. Environ. Civ. Eng.* 17 (2013) 293–314.
- [37] J.A. Schwarz, C.T. Driscoll, A.K. Bhanot, The zero point of charge of silica-alumina oxide suspensions, *J. Colloid Interface Sci.* 97 (1984) 55–61.
- [38] I. Langmuir, The adsorption of gases on plane surfaces of glass, mica and platinum, *J. Am. Chem. Soc.* 40 (1918) 1361–1403.

- [39] H.M.F. Freundlich, Over the adsorption in solution, *J. Phys. Chem.* 57 (1906) 385–470.
- [40] M.M. Dubinin, L.V. Radushkevich, Equation of the characteristic curve of activated charcoal, *Chem. Zentralbl.* 1 (1947) 875–890.
- [41] M.J. Temkin, V. Pyzhev, Recent modifications to Langmuir isotherms, *Acta Phys. Chim. URSS* 12 (1940) 217–225.
- [42] S. Lagergren, About the theory of so-called adsorption of soluble substances, *Kungliga Svenska Vetensk Handl.* 24 (1898) 1–39.
- [43] Y.S. Ho, G. McKay, Pseudo-second order model for sorption processes, *Process Biochem.* 34 (1999) 451–465.
- [44] W.J. Weber, J.C. Morris, Kinetics of adsorption on carbon from solution, *J. Sanit. Eng. Div. Am. Soc. Civ. Eng.* 89 (1963) 31–60.
- [45] G.E. Boyd, A.W. Adamson, L.S. Myers, The exchange adsorption of ions from aqueous solutions by organic zeolites. *II. Kinetics*, *J. Ame. Chem. Soc.* 69 (1947) 2836–2848.